Efficient inner filter effect of gold nanoparticles on the fluorescence of CdS quantum dots for sensitive detection of melamine in raw milk

ARTICLE *in* FOOD CONTROL · NOVEMBER 2013

Impact Factor: 2.81 · DOI: 10.1016/j.foodcont.2013.04.016

9 AUTHORS, INCLUDING:

Xianyi Cao

10 PUBLICATIONS **136** CITATIONS

SEE PROFILE

Fei Shen

Jilin University

16 PUBLICATIONS **104** CITATIONS

SEE PROFILE

Minwei Zhang

Technical University of Denmark

15 PUBLICATIONS **175** CITATIONS

SEE PROFILE

Food Control 34 (2013) 221–229

Contents lists available at SciVerse ScienceDirect

Food Control

journal homepage: www.elsevier.com/locate/foodcont

Efficient inner filter effect of gold nanoparticles on the fluorescence of CdS quantum dots for sensitive detection of melamine in raw milk

Xianyi Cao [a,1], Fei Shen [a,1], Minwei Zhang [a], Jiajia Guo [a], Yeli Luo [a], Xing Li [a], Han Liu [a], Chunyan Sun [a,*], Jingbo Liu [b,**]

[a] Department of Food Quality and Safety, College of Quartermaster Technology, Jilin University, Changchun 130062, China
[b] Department of Food Science and Engineering, College of Quartermaster Technology, Jilin University, Changchun 130062, China

ARTICLE INFO

Article history:
Received 31 January 2013
Received in revised form
8 April 2013
Accepted 10 April 2013

Keywords:
Inner filter effect
Fluorescence
Gold nanoparticles
CdS quantum dots
Melamine
Milk

ABSTRACT

A simple, rapid and ultra-sensitive analytical method for the determination of melamine in raw milk based on inner filter effect (IFE) of Au nanoparticles (AuNPs) on the fluorescence of CdS quantum dots (QDs) is described in this study. With the presence of citrate-stabilized AuNPs, the fluorescence of L-cysteine (L-Cys)-capped CdS QDs was remarkably quenched by AuNPs via IFE. The fluorescence of the AuNPs-CdS QDs system was recovered upon addition of melamine, since melamine could induce the aggregation of AuNPs accompanying the reduction of their characteristic plasmon absorption at ~522 nm, which resulted in "turn-on" of the IFE-decreased fluorescence of CdS QDs. Under the optimum conditions, a good linear correlation for detection of melamine in raw milk was exhibited from 0.05 $mg \cdot L^{-1}$ to 0.35 $mg \cdot L^{-1}$, and the detection limit was 0.017 $mg \cdot L^{-1}$, which was much lower than the detection limit of HPLC coupled with UV detector and the safety limit required by USA, UK and China. This method was successfully carried out for the assessment of melamine in raw milk samples, which revealed many advantages such as high sensitivity, low cost and non-time-consuming compared with traditional methods.

1. Introduction

As an important nitrogen-heterocyclic organic chemical raw material, melamine (1,3,5-triazine-2,4,6-triamine) is widely used for the production of melamine-formaldehyde resins. Melamine is not allowed to be used for food processing or food additives. In recent years, however, excessive melamine in raw milk and dairy products has been a worldwide concern. Especially, in 2008, Chinese dairy industry and consumer confidence were greatly devastated by the Sanlu Milk Incident which was originated from melamine-tainted milk (Qiao, Guo, & Klein, 2010). Owing to its high nitrogen level (66% by mass) and low cost, melamine was illegally adulterated in milk products, pet foods and animal feeds to increase the apparent content of crude protein and cheat quality inspectors, since the protein levels were frequently estimated by the conventional standard Kjeldahl or Dumas tests without identifying nitrogen sources. Addition of 1% of melamine in food can cause protein content artificially boosting more than 4%. Melamine in food will cause serious damage to the organs of animals or human beings. The metabolism of melamine *in vivo* is an inert metabolism, so it has low oral acute toxicity. However, melamine can be hydrolyzed to cyanuric acid which in turn associates with melamine to form reticulations, resulting in the formation of highly toxic concretions (Kobayashi et al., 2010). A long-term intake of melamine-adulterated food can induce renal malfunction and even death, especially for babies and small pets. The US Food and Drug Administration have set safety limits of melamine in adult food and infant formula as 2.5 ppm and 1.0 ppm, respectively.

Traditional analytical methods for melamine such as HPLC (Sun, Wang, Ai, Liang, & Wu, 2010), GC–MS (Goodman & Neal-Kababick, 2008), LC–MS (Goscinny, Hanot, Halbardier, Michelet, & Van Loco, 2011), ELISA (Lutter et al., 2011) and capillary electrophoresis (Xia et al., 2010), require expensive instrumentation, professional operator, complicated sample pretreatment and considerable time, therefore their application in on-site rapid detection is greatly limited. Recently, different types of methods including electrochemistry (Khlifi, Gam-Derouich, Jouini, Kalfat, & Chehimi, 2013), infrared spectroscopy (Xu, Wang, Wu, & Zhang, 2010), surface

* Corresponding author. Tel.: +86 431 87836375; fax: +86 431 87836391.
** Corresponding author. Tel.: +86 431 87836351; fax: +86 431 87836391.
E-mail addresses: sunchuny@jlu.edu.cn, sunchy814@yahoo.com.cn (C. Sun), ljb168@jlu.edu.cn, ljb168@sohu.com (J. Liu).
[1] First two authors contributed equally to this work.

0956-7135/$ – see front matter © 2013 Elsevier Ltd. All rights reserved.
http://dx.doi.org/10.1016/j.foodcont.2013.04.016

enhanced Raman spectroscopy (SERS) (Zhang et al., 2010), colorimetric sensor based on polydiacetylene (PDA) liposomes (Lee, Jeong, & Kim, 2011) *etc.*, have been developed to detect melamine in milk, but most of them suffer from complex chemical synthesis, high cost, or poor sensitivity. Consequently, investigating a rapid, accurate, simple and convenient analytical method for melamine determination has become extremely useful and profound. With the rapid development of nanotechnology, some novel methods for detecting melamine in milk have been exploited. For example, Au and Ag nanoparticles (NPs) as colorimetric probes for melamine sensing in liquid milk and infant formula have received extensive attention, due to their unique size-dependent and interparticle-distance-dependent optical properties, and the accompanying visually-obvious color change of solution (Ai, Liu, & Lu, 2009; Han & Li, 2010; Li, Li, Cheng, & Mao, 2010; Liang et al., 2011; Ping et al., 2012).

In the past two decades, quantum dots (QDs) have attracted great research interests due to their novel optical properties, such as broad excitation spectra, narrow and tunable emission spectra, high photobleaching threshold and excellent chemical stability. Some fluorescent competitive assays for detection of ions (Wang & Guo, 2009; Xue, Wang, Wang, Chen, & Tang, 2011), small molecule (Tang et al., 2008) and protein (Oh et al., 2005) have been reported based on fluorescence resonance energy transfer (FRET), with QDs acting as a desirable fluorescent donor and AuNPs as an excellent absorbant to substitute traditional organic dyes and quenchers. A sensitive and efficient method for detection of melamine has been developed based on tuning of FRET efficiency between AuNPs and CdTe-doped silica nanoparticles due to the competitive adsorption of AuNPs between CdTe-doped silica nanoparticles and melamine (Gao, Ye, Cui, & Zhang, 2012). However, the conformation of the FRET progress requires a particular distance between AuNPs and QDs to ensure the valid interaction. Therefore, establishment of FRET-based sensors usually demands sophisticated surface-chemical modification of the adoptive AuNPs or QDs, which markedly makes the detecting process very time-consuming, costly and cumbersome, and further weakens the practicality.

Herein, based on the inner filter effect (IFE) of AuNPs on the fluorescence of L-cysteine (L-Cys)-capped CdS QDs, we demonstrate a simple, sensitive and reliable melamine sensing system for milk which is different from the above AuNPs/QDs-based FRET detecting system. The superiority of this approach lies in unrequirement of the specific modification of AuNPs or QDs, thus the detecting process becomes more flexible and simple by only utilizing the two materials as such. Recent fluorescence analyses show more novel applications based on IFE, such as for detection of Al^{3+} (Wang, Xiong, Geng, Zhang, & Xu, 2011), aminothiol (Xu, Li, & Jin, 2011) and cyanide (Shang & Dong, 2009). The mechanism of IFE refers to the absorption of the excitation and/or emission light of fluorophore by absorber in the detection system. Specifically, when the absorption spectrum of the absorber has an overlap with the excitation and/or emission spectrum of the fluorophore, the fluorescence emission of the fluorophore will be tuned by the mutative absorption of the absorber. Thus the absorption response of the chemosensor to analyte will be precisely and effectively converted to the fluorescence signal, which makes fluorescence analysis of the analyte feasible. Since the changes in the absorbance of the absorber transform into the fluorescence changes of the fluorophore exponentially, an enhanced sensitivity for the detection of the analyte is achieved with respect to the absorbance of the absorber alone (Shao et al., 2005).

The principle of the proposed method is illustrated in Scheme 1. The as-prepared citrate-stabilized AuNPs are claret-red and well dispersed (1). Due to the strong absorption of AuNPs at 522 nm, the fluorescence of CdS QDs is obviously quenched in the presence of citrate-stabilized AuNPs via IFE (2). Upon addition of melamine,

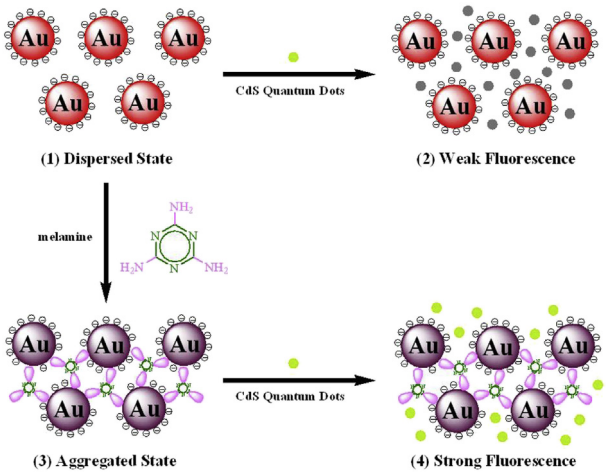

Scheme 1. Schematic illustration of the turn-on fluorescent detection of melamine based on the inner filter effect of AuNPs on L-Cys-capped CdS QDs.

AuNPs will aggregate and the absorption at 522 nm is diminished, as melamine would strongly bind to the surface of AuNPs through the amine groups by the ligand exchange with citrate ions (Li et al., 2010) which rapidly and strongly decreases the stability of the AuNPs (3). Hence the fluorescence of CdS QDs is variously recovered when different concentrations of melamine was added (4). The recovery of the fluorescence intensity illustrated a good linear dependence on melamine concentration at ppb level. Generally, an adequate collaboration of absorber/fluorophore is very difficult to find and establish, since an effective IFE would occur only if a broad overlap exists between the absorption band of the absorber and the excitation and/or emission bands of the fluorophore. Thanks to their excellent characteristics, such as extremely large extinction coefficient (about 10^8 $M^{-1}\cdot cm^{-1}$ or more) and flexibly tuned absorption spectrum, AuNPs can be utilized as extraordinarily effective absorber in IFE-based fluorescence assay (Shang & Dong, 2009). Moreover, due to their superior optical properties, QDs can perform the role of potentially ideal fluorophore (Zhang et al., 2012). By using the above two materials, the whole detection process for melamine including pretreatment procedure could be conveniently and simply completed within a short period of time. Therefore, rapid and reliable on-site screening of melamine in milk would be promisingly achieved.

2. Experimental

2.1. Reagents and materials

$AuCl_3\cdot HCl\cdot 4H_2O$, sodium citrate, citric acid, ammonia water, $FeCl_3$, NaCl, $MgCl_2$, $ZnCl_2$, KCl, Na_3PO_4, NaOH, Na_2CO_3, glucose, vitamin C and isopropyl alcohol were purchased from Beijing Chemical Reagent Company (Beijing, China). Vitamin B_1, vitamin B_2, glysine, L-cysteine, L-histidine, L-tryptophan, L-threonine and L-lysine were obtained from Huishi Biochemical Reagent Company (Shanghai, China). Sodium sulfide ($Na_2S\cdot 9H_2O$), $CaCl_2$ and trichloroacetic acid were purchased from Xilong Chemical Co., Ltd (Shantou, China). Cadmium chloride ($CdCl_2\cdot 2.5H_2O$) was purchased from Sinopharm Chemical Reagent Co., Ltd (Shanghai, China). Melamine and lactose were purchased from Aladdin Reagent Company (Shanghai, China). CH_3OH (chromatographic grade) was obtained from TEDIA Company, Inc (Fairfield, USA). Acetonitrile and sodium 1-octanesulphonate (chromatographic grade) were purchased from Yuwang Chemical Reagent Company (Yucheng, China). Unless otherwise stated, all the chemicals were of analytical

grade. High purity nitrogen (99.999%) and triply distilled water (TDW) were used in all experiments. The liquid raw milk was purchased from a local pasture which is one of qualified suppliers of a famous dairy enterprise. The main composition of the liquid raw milk is substantially as follows: moisture 87.6%, protein 3.4%, carbohydrate (lactose mostly) 4.8%, fat 3.3%, mineral 0.8% and vitamin 0.1%.

Melamine standard stock solution for HPLC test was easily prepared as follows: In a 100 mL volumetric flask, 100 mg of melamine was dissolved with 50% (v/v) methanol aqueous solution, and then the solution was diluted to 100 mL, to obtain a 1 $mg \cdot mL^{-1}$ standard stock solution, which was stored at 4 °C in a dark place. The stock solution was respectively diluted to 0.8, 2, 20, 40, 80 μg/mL with mobile phase to obtain working solutions.

HPLC mobile phase was a mixture of solution A (90%) and solution B (10%). Solution A was prepared as follows: 2.10 g of citric acid and 2.16 g of sodium 1-octanesulphonate were dissolved with 980 mL of TDW. Then the pH of the solution was adjusted to 3.0 with 1 M NaOH, and the solution was diluted to 1 L with TDW. Solution B was acetonitrile (chromatographic grade). Solution A and B were mixed in proportion, filtered through a PVDF filter membrane of 0.2 μm and supersonicated for 30 min to exclude air bubbles before use.

2.2. Apparatus

Transmission electron microscopy (TEM) measurements were made on a TECNAI F20 (FEI Co., Holland) operated at an accelerating voltage of 200 kV. Fourier transform infrared spectra (FTIR) were recorded with an IRPrestige-21 FTIR spectrometer (Shimadzu, Tokyo, Japan). The absorption spectra were recorded on a 2550 UV–vis spectrophotometer (Shimadzu, Tokyo, Japan). The fluorescence spectra were acquired on a RF-5301PC fluorescence spectrophotometer (Shimadzu, Tokyo, Japan) at the excitation wavelength of 360 nm, with both of the exciting and emission slits set at 5 nm. The fluorescence lifetime measurements were conducted using a FLS 920 spectrometer (Edinburgh Instruments, UK). Zeta potential (ζ) was performed on a Zeta Sizer Nano ZS particle analyzer. The HPLC system consisted of a Shimadzu LC-2010AHT liquid chromatograph, a SPD-20A UV detector and a C18 column (250 mm × 4.6 mm, 5 μm, i.d.) with a data acquisition software of LC solution (Shimadzu, Tokyo, Japan). The operation conditions were as follows: injection volume, 20 μL; detection wavelength, 240 nm; flow rate, 1.0 $mL \cdot min^{-1}$; total running time, 25 min. Solid phase extraction (SPE) was carried out on a QSE-12 SPE system (Huaruiboyuan, Beijing, China) equipped with PCX-SPE columns (60 mg, 3 mL, Simon Aldrich, Germany). Nitrogen blowing was performed on a MD-12 nitrogen blowing instrument (Tapery, Nanjing, China). The ultrasonic treatment was carried out on a 125 KQ-300DE ultrasonicator (Kunshan, Shanghai, China). The centrifugation was performed on a CR20B2 refrigerated centrifuge (Hitachi, Tokyo, Japan). Magnetic stirring was carried out on a GL-3250B magnetic stirrer (QILINBEIER, Haimen, China). Vortex mixing was performed on a WH-3 vortex mixer (Huxi, Shanghai, China). All pH measurements were carried out with a Model pHS-3C (Chenghua, Shanghai, China). All optical measurements were performed at room temperature under ambient conditions.

2.3. Synthesis and characterization of AuNPs

The colloidal citrate-stabilized AuNPs of 13 nm in diameter were prepared using Frens' method described in a previous report (Grabar et al., 1997). All pieces of glassware were cleaned with newly prepared aqua regia, rinsed completely with triple distilled water and dried thoroughly before synthesis. Typically, in a 250 mL round-bottom flask equipped with a reflux condenser under continuous magnetic stirring, 10 mL of sodium citrate (38.8 mM) was quickly injected into 100 mL vigorous boiling solution of $HAuCl_4$ (1 mM) with a syringe. After the appearance of a color change from pale yellow to deep red, the mixture solution was refluxed for an additional 10 min under stirring. Then the heating equipment was removed, and stirring was continued for another 15 min. The solution naturally cooled down to room temperature, and it was filtered through a 0.4 μm Millipore filter membrane and then stored at 4 °C. The size and morphology of as-prepared AuNPs were characterized with TEM, and the particle diameter is about 13 ± 1.4 nm. The molar extinction coefficient (ε) at ~520 nm for the 13 nm AuNPs is about $2.7 \times 10^8\ M^{-1} \cdot cm^{-1}$ (Zhao, Brook, & Li, 2008), thus the molar concentration of the AuNPs was calculated to be nearly 7.0×10^{-9} M according to Lambert Beer's law. The as-prepared AuNPs colloid was diluted with TDW to 1.4×10^{-9} M for further use.

2.4. Synthesis, purification and characterization of water-soluble L-Cys-capped CdS QDs

The water-soluble L-Cys-capped CdS QDs were easily prepared in a simple procedure (Weon, Rizwana, & Rajesh, 1998) as follows: an accurate weight of $CdCl_2$ was dissolved in 15 mL of TDW, which had been purged with pure nitrogen gas for 60 min, to obtain 0.01 M Cd^{2+} solution. Then 30 mL of 0.01 M L-Cys aqueous solution was slowly added at room temperature, resulting in a L-Cys/Cd^{2+} molar ratio of 2:1. 1 M NaOH was used to adjust the pH value of the solution to 8.5–9.0. After purging the mixture with pure nitrogen gas for another 60 min, 15 mL of 0.01 M freshly prepared Na_2S was added dropwise into the vortex of the solution with a syringe to reach Cd^{2+}/S^{2-} molar ratio of 1:1. The bright yellow colloid was sealed to incubate for 2 h at 50 °C, and cooled down to room temperature to incubate for another 6 h. All steps were carried out under continuous magnetic stirring. The colloid solution was stored at 4 °C in a brown reagent bottle (narrow mouth). This crude CdS QDs colloid solution was washed with equal isopropyl alcohol and centrifuged to remove excess precursors. Then the QDs deposit was dried by a vacuum drier. Finally, the prepared L-Cys-capped CdS QDs were dispersed in water again for further use.

The particle feature of the L-Cys-capped CdS QDs could be tuned by adopting different reaction conditions, such as the molar ratios and concentrations of reactants and the reaction temperature. In this work, based on evaluation for several different reaction conditions, the molar ratio of Cd^{2+}/L-Cys/S^{2-}, the concentration of $CdCl_2$ and the reaction temperature were optimized to be 1:2:1, 2.5 mM and 50 °C, respectively, which resulted in relatively high product yield, adequate quantum yield and good analytical performance in this detecting system.

According to the calculation method mentioned in a previous research (Yu, Qu, Guo, & Peng, 2003), the particle sizes of the obtained L-Cys-capped CdS QDs were calculated by the following empirical formula: $D = (-6.6521 \times 10^{-8})\lambda^3 + (1.9557 \times 10^{-4})\lambda^2 - (9.2352 \times 10^{-2})\lambda + 13.29$ (nm). In this formula, D (nm) is the particle size of a given QDs sample, and λ (nm) is the wavelength of the first excitonic absorption peak of the corresponding QDs. The molar concentration of the as-prepared L-Cys-capped CdS QDs was calculated using the Lambert Beer's law $A = \varepsilon cl$, where A is the absorbance of the first excitonic absorption peak of the corresponding QDs, c is the molar concentration (M) of the QDs solution, l is the path length (cm) of the radiation beam used for recording the absorption spectrum and was set at 1.0 cm here, and ε is the molar extinction coefficient of CdS QDs at the first excitonic absorption peak. According to the previous literature (Yu et al., 2003), ε could be obtained by the following formula $\varepsilon = 21{,}536\,(D)^{2.3}$, in which D (nm)

is the particle size of the QDs sample. Thus the molar concentration of the QDs solution was calculated to be 4.67×10^{-6} M according to the above formulas. The as-prepared CdS QDs solution was diluted with TDW to 2.33×10^{-6} M for further use.

2.5. Fluorescence detection of melamine

The fluorescence emission spectra were recorded with the excitation of 360 nm, and the slit widths of excitation and emission are 5 nm in all tests. Typically, in a 5 mL test tube, 1 mL CdS QDs (2.33×10^{-6} M, pH = 7.0) were mixed respectively with 1 mL different concentrations of AuNPs at room temperature, and then the mixture was diluted to 3 mL with TDW and mixed thoroughly. The fluorescence emission spectra of the solutions were recorded and analyzed to evaluate the most suitable concentration of AuNPs (1.63×10^{-10} M in the 3 mL sample solution). Afterwards, 1 mL of optimized-concentration AuNPs solution was mixed with 1 mL of melamine solution with different concentrations, and the mixture was incubated at room temperature for 10 min. Then, 1 mL of 2.33×10^{-6} M CdS QDs was added into the above mixture. The obtained mixture was also diluted to 3 mL with TDW and mixed thoroughly. The fluorescence data were analyzed by plotting the fluorescence spectra, and the calibration curve for melamine was set up according to the increased fluorescence intensity, $\Delta F = F - F_0$, where F and F_0 are the maximum emission intensity of the system in the presence and absence of melamine, respectively.

2.6. Detection of melamine in raw milk

The extraction of the raw milk for the detection of melamine was carried out according to the method stipulated by Chinese National Standard GB/T 22388-2008. In a 50 mL centrifuge tube, 2 g (±0.01 g) of raw milk was mixed with 15 mL of 1% (w/v) trichloroacetic acid and 5 mL acetonitrile. The mixture was respectively ultrasonically-treated and vibratively-extracted for 10 min to deposit protein and dissolve organic substances. Then the mixture was centrifuged at 12,000 rpm for 10 min to separate the deposit, and the supernatant was filtered through a filter paper soaked by 1% (w/v) trichloroacetic acid. The pH of the filtrate was adjusted to 7.0 by using 1 M Na_2CO_3. The solution was diluted with TDW to 25 mL to obtain the final solution, which was used for determination according to the proposed method in Section 2.5. A certain amount of melamine was doped into the raw milk, then pretreated and analyzed in accordance with the above procedure.

For the measurement of HPLC, the above final solution needs to be further purified by SPE columns as follows: The SPE column was firstly activated with 3 mL of methanol and 5 mL of TDW respectively. Then the mixture of 5 mL of the final solution and 5 mL of TDW was passed through the column. After continuous washing with 3 mL of water and 3 mL of methanol, the column was dried approximatively under negative pressure for 3 min and finally eluted with 6 mL of 5% (v/v) ammonium hydroxide in methanol. The flow rate was no more than 1 mL·min^{-1} in the whole process. The eluent was collected and dried under nitrogen at 50 °C and the residue was redissolved in 1 mL of mobile phase solution. The solution of residue was filtered through a 0.2 μm PVDF filter membrane to obtain the final HPLC sample.

3. Results and discussion

3.1. Characteristics of AuNPs and L-Cys-capped CdS QDs

The UV–vis absorption spectrum of the colloidal citrate-stabilized AuNPs was obtained by scanning the solution in the wavelength range from 300 to 700 nm. Shown as the curve a in Fig. 1, the claret-red aqueous solution of the citrate-stabilized AuNPs displays a strong characteristic plasmon absorption (λ_{max} = 522 nm). The average diameter of the as-prepared well-dispersed AuNPs was observed about 13 nm according to the TEM image.

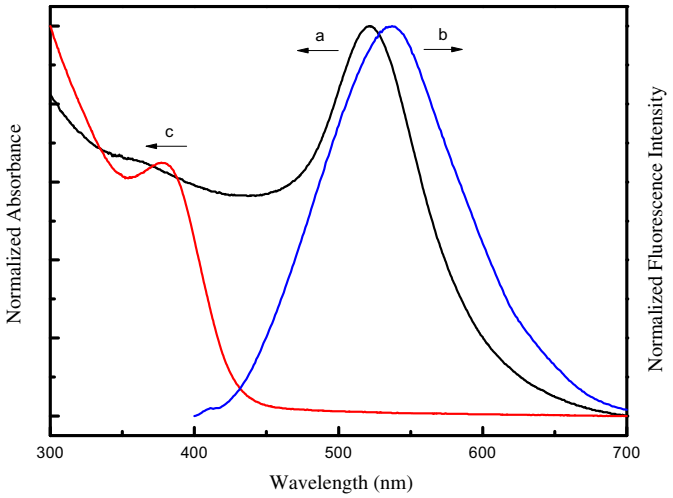

Fig. 1. Absorption spectrum of AuNPs (a), fluorescence emission spectrum of L-Cys-capped CdS QDs (b) and absorption spectrum of L-Cys-capped CdS QDs (c).

Water-soluble L-Cys-capped CdS QDs were directly synthesized in aqueous phase, and the obtained CdS QDs show a maximum fluorescence emission at 537 nm (curve b in Fig. 1). The particle size of the L-Cys-capped CdS QDs was difficult to be characterized by TEM due to their small dimensions and trend to aggregate when drying on a Cu grid (Xue et al., 2011), therefore other characterization methods were considered. The absorption spectrum of the CdS QDs (curve c in Fig. 1) indicated that the average particle size of the as-prepared QDs was about 2.8 nm, and the concentration of QDs is about 4.67×10^{-6} M, derived from the wavelength of the first excitonic absorption peak (λ_{max} = 377 nm) based on the empirical fitting functions mentioned in Section 2.4.

To identify the conjugation mode between L-Cys and CdS QDs, the IR spectra of pure L-Cys and L-Cys-capped CdS QDs were measured and shown in Fig. 2. The similarity in both spectral characteristics and several peak positions proves that L-Cys was well chemically-attached onto the surface of the CdS QDs. On the other hand, the conjugation mode of L-Cys and CdS QDs can be

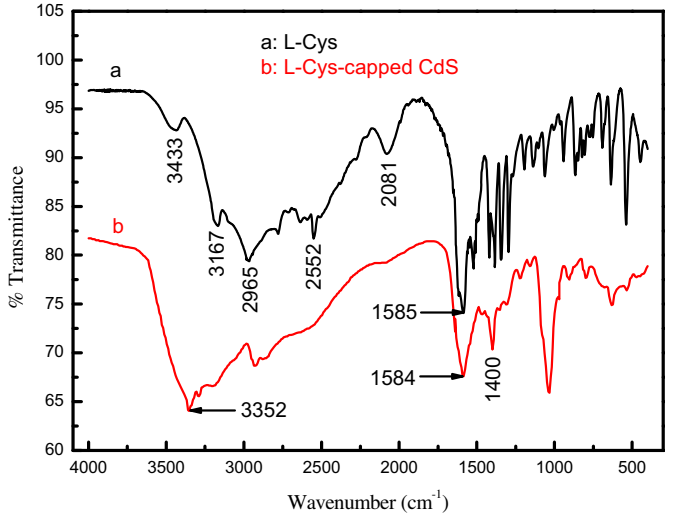

Fig. 2. IR spectra of L-Cys (a) and the L-Cys-capped CdS QDs (b).

confirmed by some distinctive differences between the two spectra. The absorption peaks around 1390–1400 cm^{-1} ($m\upsilon COO^-$) and 1580–1590 cm^{-1} ($s\upsilon COO^-$) represent –COO group. The observed features around 2070–2090 cm^{-1} ($w\upsilon N–H$), 2700–3200 cm^{-1} ($s\upsilon N–H$) and 2530–2650 cm^{-1} ($m\upsilon N–H$) indicate $-NH_3^+$ group. The peak around 3430–3450 cm^{-1} ($m\upsilon N–H$) points out $-NH_2$ group, while the absorption band around 2550–2670 cm^{-1} ($w\upsilon S–H$) indicates –SH group. There are coexisting absorption bands of $-COO^-$, $-NH_3^+$ and –SH on pure L-Cys (curve a in Fig. 2), whereas only absorption bands of $-COO^-$ and $-NH_2$ were observed on the L-Cys-capped CdS QDs (curve b in Fig. 2). The disappearance of S–H vibration around 2550–2670 cm^{-1} on the L-Cys-capped CdS QDs could be attributed to the conformation of covalent bonds between thiols and the surface of CdS QDs. The bands of $-NH_2$ group present on the L-Cys-capped CdS QDs can be ascribed to the basification of $-NH_3^+$ group of L-Cys under pH 7.0.

3.2. Effects of AuNPs on the fluorescence of L-Cys-capped CdS QDs

As shown in Fig. 1, it is obvious that the emission maximum of CdS QDs is just extraordinarily near the absorption maximum of AuNPs, and the absorption spectrum of AuNPs overlaps well with the fluorescence emission spectrum of CdS QDs. Thus, if the two materials coexist, the effective emission intensity of CdS QDs might be substantially decreased or even entirely quenched. It can be seen from Fig. 3 that the fluorescence emission intensity of CdS QDs decreases gradually upon increasing the concentration of AuNPs. According to a previous report (Grabar et al., 1997; Li et al., 2010), due to the negative capping agent's (citrate ion) electrostatic repulsion against van der Waals attraction between AuNPs, the colloidal citrate-stabilized AuNPs can be stabilized against aggregation. Therefore, the surface of AuNPs possesses negative charges, which was further supported by the zeta potential data of AuNPs (Fig. S1A). The dispersed ~13 nm AuNPs (pH = 7.0) displayed the zeta potential of −28.9 mV. The zeta potential of the CdS QDs (pH = 7.0) was measured to be −20.4 mV (Fig. S1B), due to the ionization of the –COOH group in L-Cys (pI = 5.02). Since both AuNPs and CdS QDs possess negative charges, there is no electrostatic attractive interaction between them. It has been proved that the positively charged QDs and the negatively charged AuNPs could form FRET donor-acceptor assemblies by electrostatic interactions, in which the fluorescence intensity of QDs was effectively quenched, since the electrostatic interaction could curtail the distance between the QDs donor and the AuNPs acceptor (Wang & Guo, 2009). Besides, as a triprotic acid, citric acid has three pKa values: 3.13, 4.76 and 6.40. So it could be deduced that an effective FRET donor-acceptor assembly could be hardly established due to the hydrogen bond formed between L-Cys-capped QDs and citrate-capped AuNPs herein, because –COOH group in citric acid was almost deprotonated in neural aqueous solution (pH = 7.0) (Xue et al., 2011). It is obvious that in the present work (pH = 7.0), an efficient FRET process did not occur due to electrostatic interaction or hydrogen bonds between the negatively charged AuNPs and the negatively charged CdS QDs.

As a parameter which is hardly influenced by IFE, static quenching and variations in the fluorophore concentration, fluorescence lifetime is usually used to confirm that an efficient FRET process occurs because non-radiative energy transfer is expected to essentially change the exciton lifetime of the donor. As shown in Fig. S2, the average lifetime of L-Cys-capped CdS QDs was hardly changed in the presence of AuNPs. This result further suggested that the quenched emission of the CdS QDs by AuNPs was not due to the FRET between AuNPs and CdS QDs. Furthermore, no complex formation or energy transfer was observed between AuNPs and CdS QDs in this detecting system, which was supported by the fact that the plasmon absorption band of AuNPs itself remained unchanged in the presence of CdS QDs. Therefore, the observed fluorescence decrease should be mainly attributed to the IFE of AuNPs on the fluorescence of CdS QDs.

With increasing the concentration of AuNPs, the absorbance of the absorber increased, which would effectively weaken the emission light from CdS QDs. As a result, the emission intensity of CdS QDs gradually decreased or even completely quenched. Notably, due to high extinction coefficient of AuNPs, the fluorescence intensity of 7.78×10^{-7} M CdS QDs decreased by over 75% in the presence of 1.63×10^{-10} M AuNPs. Therefore, the fluorescence of CdS QDs at 537 nm can be modulated by the absorbance of AuNPs via IFE in a sensitive and simple approach. Compared to the complicated and costly process to construct QDs-AuNPs FRET assemblies (Dyadyusha et al., 2005; Oh et al., 2005; Tang et al., 2008), this kind of IFE mechanism is very practical.

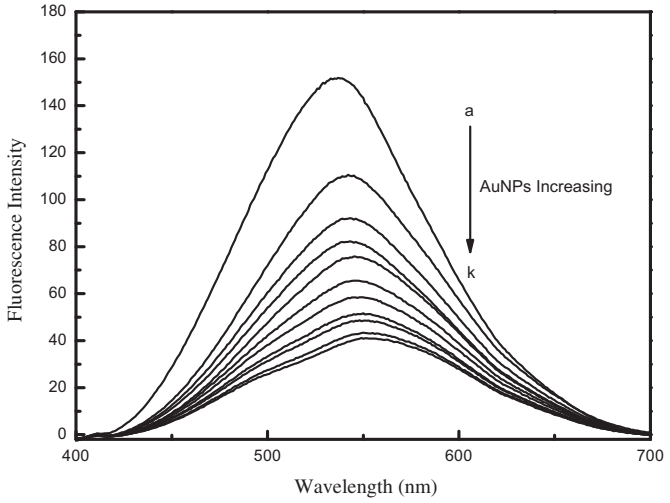

Fig. 3. Fluorescence emission spectra of L-Cys-capped CdS QDs in the presence of increasing concentrations of AuNPs. The concentration of AuNPs in samples (a)-(k) is 0, 0.23, 0.47, 0.70, 0.93, 1.17, 1.40, 1.63, 1.87, 2.10 and 2.33×10^{-10} M, respectively. CdS QDs, 7.78×10^{-7} M.

3.3. Effects of melamine on the optical characteristics of AuNPs

The UV–vis absorption spectra changes of AuNPs induced by melamine were recorded and shown in Fig. 4A. Upon the increasement of melamine concentration, the absorbance of AuNPs at 522 nm gradually decreased, with the red shift and broadening of the surface plasmon band of AuNPs, while inducing an accompanying color change of AuNPs solution from red to purple. Some previous researches have confirmed that the surface plasmon absorption of AuNPs is very sensitive to their interparticle distance. As the interparticle distance decreases, the first peak becomes gradually weak, and the second red-shifted plasmon absorption peak comes out owing to the aggregation of AuNPs when the individual nanoparticles are electronically attached to each other (Link & El-Sayed, 1999). As shown in Scheme 1, melamine could strongly bind to the surface of AuNPs through the amine groups by the ligand exchange with citrate ions, and the ligand exchange decreases the electrostatic repulsion among individual nanoparticles and finally results in the aggregation of AuNPs (Guo et al., 2010; Li et al., 2010). Besides, due to NH···N hydrogen bonds between melamine molecules, the neighbor melamine-coated AuNPs could also be cross-linked, thus inducing the aggregation of AuNPs (Li et al., 2010).

Melamine-induced aggregation of AuNPs was further confirmed by the TEM images: Fig. 4B and C respectively revealed well-

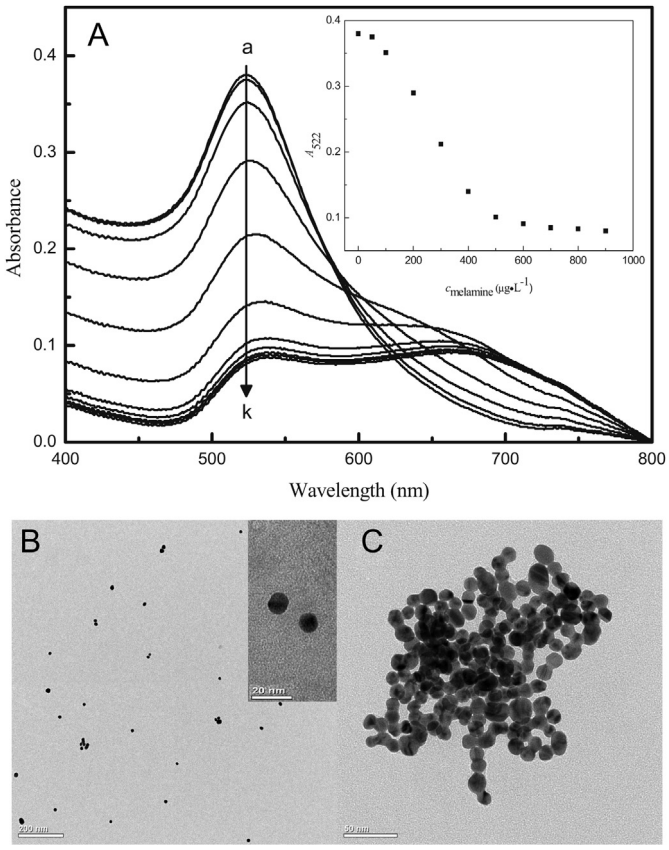

Fig. 4. (A) Absorption spectra of AuNPs (1.63×10^{-10} M) in the presence of melamine at various concentrations. The melamine in samples (a)-(k) is 0, 50, 100, 200, 300, 400, 500, 600, 700, 800 and 900 μg·L^{-1}, respectively. The inset shows the absorbance at 522 nm *versus* the concentration of melamine. (B) TEM image of AuNPs. (C) TEM image of AuNPs after addition of melamine.

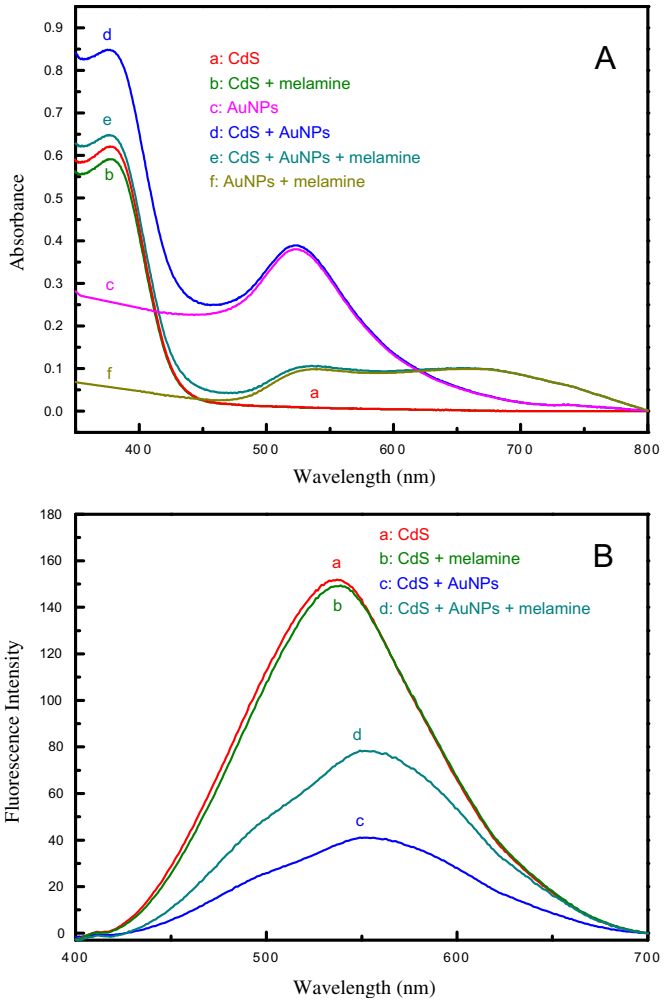

Fig. 5. (A) Absorption spectra: a, CdS QDs; b, CdS QDs and melamine; c, AuNPs; d, CdS QDs and AuNPs; e, CdS QDs, AuNPs and melamine; f, AuNPs and melamine; (B) Fluorescence emission spectra: a, CdS QDs; b, CdS QDs and melamine; c, CdS QDs and AuNPs; d, CdS QDs, AuNPs and melamine. CdS QDs, 7.78×10^{-7} M; melamine, 600 μg·L^{-1} (A) and 35 μg·L^{-1} (B); AuNPs, 1.63×10^{-10} M.

dispersed nanoparticles in the absence of melamine and aggregation of AuNPs in the presence of melamine. The results were accordant with the spectra changes in Fig. 4A. Therefore, the fluorescence emission of L-Cys-capped CdS QDs centered at 537 nm can be regulated in the melamine-AuNPs detecting system via IFE, which provides a novel and feasible way for fluorescent detection of melamine. In fact, the aggregation and accompanying color change of AuNPs induced by melamine have been applied for the visual sensing of melamine in liquid milk, infant and pet food (Guo et al., 2010; Li et al., 2010). However, colorimetric technique for the detection of small molecules generally displays lower sensitivity than fluorescence analytical methods. Based on the present IFE-based detecting mechanism, the tiny variation of absorption signals was converted into exponential changes in fluorescence signals, which is very hopeful to greatly ameliorate the detecting sensitivity and lower the detection limit in a simple way.

3.4. IFE-based AuNPs-QDs emission response to melamine

Considering the molecular bonding between melamine and AuNPs and the significant change of fluorescence emission of CdS QDs quenched by AuNPs via IFE, it is reasonable to expect that the IFE of AuNPs on CdS QDs would be affected by melamine, which aggregates the AuNPs and modulates the IFE process (Scheme 1), and the IFE-based QDs emission would respond to melamine concentration. To verify this expected detecting principle for melamine, the effects of melamine on the absorption and fluorescence spectra of AuNPs-QDs are shown in Fig. 5. The absorption and fluorescence spectra (curves a in Fig. 5) of CdS QDs were identical to those of the mixture of melamine and CdS QDs (curves b in Fig. 5), which demonstrated that there was no molecular interaction between melamine and CdS QDs in this detecting system. The plasmon absorption band of AuNPs showed no obvious difference in the absence and presence of CdS QDs (curve c and curve d in Fig. 5A), illuminating that there was no molecular interaction between CdS QDs and AuNPs. Therefore, the melamine-induced changes of the plasmon absorption band of AuNPs were identical with or without the presence of CdS QDs (curve e and curve f in Fig. 5A), which illustrated that the aggregation of AuNPs induced by melamine was not disturbed by the presence of CdS QDs. When CdS QDs was mixed with AuNPs, the fluorescence emission was significantly quenched (curve c in Fig. 5B) via IFE. However, the IFE-decreased fluorescence of CdS QDs was evidently recovered with the presence of melamine (curve d in Fig. 5B). No notable change in the shape of the emission spectra of CdS QDs appeared in the presence of AuNPs-melamine, demonstrating that the recovered emission was still distributed by CdS QDs rather than any other possible newly-formed emission centers. As melamine could not promote the fluorescence intensity of the CdS QDs in the absence of AuNPs, thus it was confirmed that the fluorescence recovery should originate from the interaction between melamine and AuNPs which

then affected the fluorescence emission of the CdS QDs. Melamine could induce the absorbance decrease of the plasmon absorption band of AuNPs at 522 nm which weakened the IFE of AuNPs on CdS QDs and then lead to the recovery of the IFE-decreased fluorescence emission of CdS QDs. Due to the turn-on effect of melamine to the fluorescence of AuNPs-CdS, developing a novel, simple and sensitive IFE-based fluorescence chemosensor for rapid determination of melamine in raw milk is necessary to be further studied.

3.5. Optimization of assay conditions

The proposed melamine chemosensor is based on the molecular bonding between melamine and AuNPs, which induced decrease of the plasmon absorption band of AuNPs, and then resulted in the recovery of the fluorescence of CdS QDs. Therefore, the analytical performance of the melamine chemosensor is strongly influenced by assay conditions such as the media pH, the concentration of AuNPs and reaction time. Different assay conditions were further evaluated in our studies.

The pH of the solution has great effect on the fluorescence intensity of the system. Melamine is a weak base with a pKa of 5.05, and pH also influences the existing form of melamine in aqueous solution. As shown in Fig. S3, the effect of pH on the fluorescence recovery was investigated in the range from 5.5 to 8.5 for the detection of 35 $\mu g \cdot L^{-1}$ melamine by addition of 0.1 M NaOH or HCl. The maximum of $F - F_0$ value was obtained at pH 7.0, which is probably due to the fact that melamine could be hydrolyzed in acidic or basic to lose some or all amino groups gradually. This hydrolysis process finally caused that melamine was transformed into cyanuric acid (Li et al., 2010), and then the molecular bonding process between AuNPs and melamine was disturbed, thus no appreciable absorbance decrease of AuNPs and turn-on effect of fluorescence emission of CdS QDs was observed. Therefore, the optimal pH 7.0 was chosen for further studies.

The effect of the concentration of AuNPs on the fluorescence response toward melamine was also investigated. As shown in Fig. S4, 1.63×10^{-10} M AuNPs gave the best response in terms of both the sensitivity and linear dynamic range in the present experiment. A higher concentration of AuNPs could weaken the background fluorescence more effectively, but the response for melamine in the low concentration range was too weak which would reduce the detection sensitivity. In addition, a lower concentration of AuNPs could enhance the response for melamine in the low concentration range, but the background fluorescence would be higher which could also affect the sensitivity of the method, and the linear dynamic range was also found to be narrower.

We investigated the reaction time of melamine-AuNPs binding and AuNPs-CdS QDs interaction. The optimum incubation time for melamine-AuNPs binding (Fig. S5) was investigated by recording the absorption spectra every 30 s after addition of melamine into AuNPs solution. The results show that the aggregation of AuNPs completed within 10 min. On the other hand, after addition of CdS QDs to AuNPs solution, the fluorescence intensity of CdS QDs was immediately quenched due to the IFE of AuNPs. Therefore, the incubation time of melamine-AuNPs binding was chosen as 10 min, and no further incubation was necessary after addition of CdS QDs into the above melamine-AuNPs mixture.

Under the optimum conditions, the analytical parameters of the present method for melamine determination were then investigated. As shown in Fig. 6A, the fluorescence intensity of AuNPs-QDs increases gradually with the increment of melamine concentration, which corresponds with a gradual decrease on the plasmon absorbance of AuNPs at 522 nm (Fig. 4A). A good linear relationship between the increased fluorescence intensity ($\Delta F = F - F_0$) and the melamine concentration is obtained in the range of 7–49 $\mu g \cdot L^{-1}$

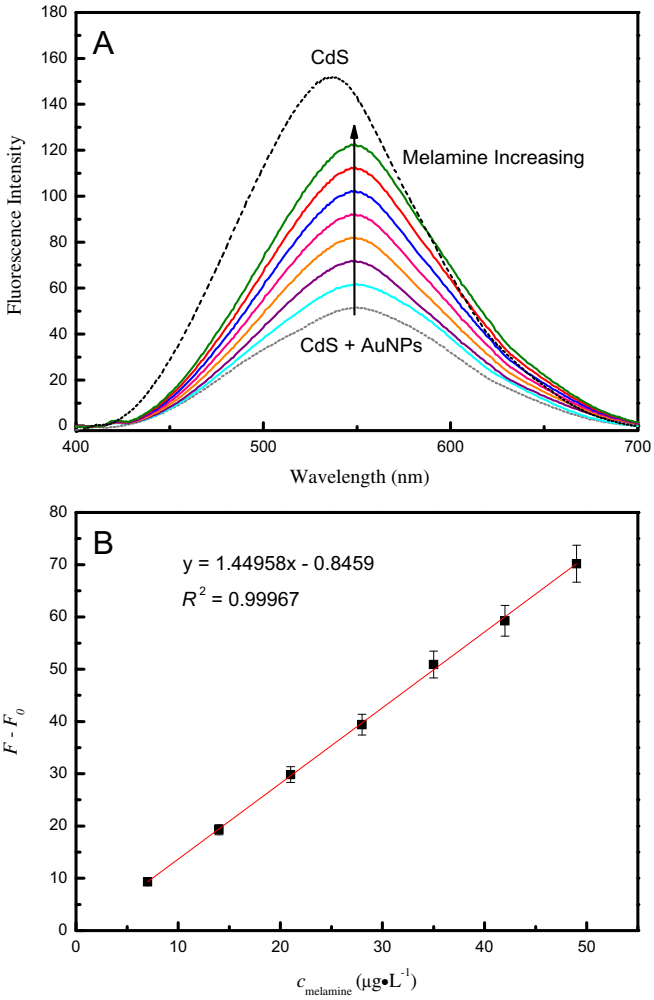

Fig. 6. Fluorescence emission spectra of AuNPs-CdS QDs system in the presence of increasing concentrations of melamine (A) and linear plot of increased fluorescence intensity ($F - F_0$) at the maximum emission wavelength *versus* the concentration of melamine (B). The concentration of melamine in samples (solid curves) is 7, 14, 21, 28, 35, 42 and 49 $\mu g \cdot L^{-1}$, respectively. CdS QDs, 7.78×10^{-7} M; AuNPs, 1.63×10^{-10} M.

($R^2 = 0.99$, Fig. 6B). The detection limit was 2.3 $\mu g \cdot L^{-1}$ (3σ). The relative standard deviation for 11 repeated measurements of 35 $\mu g \cdot L^{-1}$ melamine was 0.9%, which indicated that the fluorescence response of AuNPs-QDs toward melamine was provided with high reproducibility.

3.6. Interference studies

To assess the selectivity of the determination method for melamine, the effects of various potential interfering substances in raw milk (http://en.wikipedia.org/wiki/Milk#Nutritional_vaule) were investigated for determination of 35 $\mu g \cdot L^{-1}$ melamine. The fluorescence spectra of AuNPs-QDs with the presence of melamine premixed with different interfering substances are shown in Fig. S6A and the corresponding response are shown in Fig. S6B, in which the response for 35 $\mu g \cdot L^{-1}$ melamine without addition of any other substance is defined as 1. It can be seen that 100-fold vitamin B_1 (0.044 $g \cdot L^{-1}$), glucose (4.2 $g \cdot L^{-1}$), L-threonine (143 $g \cdot L^{-1}$), K^+ (143 $g \cdot L^{-1}$), Na^+ (43 $g \cdot L^{-1}$), Cl^- (100 $g \cdot L^{-1}$), NO_3^- (1.1 $g \cdot L^{-1}$), 50-fold glycine (37.5 $g \cdot L^{-1}$), Mg^{2+} (5 $g \cdot L^{-1}$), 10-fold L-tryptophan (7.5 $g \cdot L^{-1}$), L-lysine (14 $g \cdot L^{-1}$), L-histidine (7.5 $g \cdot L^{-1}$), vitamin C (0.0003 $g \cdot L^{-1}$), and 5-fold Ca^{2+} (5.65 $g \cdot L^{-1}$), lactose (240 $g \cdot L^{-1}$) induced less than ± 5% interference for the determination of

Table 1
Application of HPLC for the determination of melamine in raw milk samples spiked with different amounts of melamine ($n = 3$).

Sample	Concentration of melamine ($mg \cdot L^{-1}$)		Recovery (%)	RSD (%)
	Amount added	Amount found[a]		
Milk 1	2	1.98 ± 0.13	98.9	6.3
Milk 2	5	4.26 ± 0.16	85.2	3.8
Milk 3	10	8.97 ± 0.42	89.7	4.7

[a] Average value of three determinations ± standard deviation.

melamine. Thus, the AuNPs-CdS QDs detecting system herein possessed a good selective fluorescence response toward melamine and it could be applied to detect trace melamine in raw milk.

3.7. Detection of melamine in real samples

To validate the reliability of the proposed method to specifically detect melamine in real samples, known quantities of melamine were doped into the samples of raw milk before sample pretreatment and then the melamine-doped raw milk samples were analyzed according to the procedures described in Section 2.5 and Section 2.6. As shown in Fig. S7, the signal ($F - F_0$) of the assay exhibited a linear correlation to melamine concentration in raw milk in the range from 0.05 to 0.35 $mg \cdot L^{-1}$. The detection limit (3σ) is found to be 0.017 $mg \cdot L^{-1}$, which is well below the safety limit (2.5 $mg \cdot L^{-1}$ in USA and the UK; 1 $mg \cdot L^{-1}$ for infant formula in China), thus it can be indicated that our IFE-based fluorescent detection system was sensitive enough for melamine detection in raw milk. The relative standard deviation (RSD) was 2.1% for the determination of 0.1 $mg \cdot L^{-1}$ melamine ($n = 11$).

3.8. Comparison of the proposed IFE-based fluorescent assay with HPLC assay

According to Chinese National Standard GB/T 22388-2008, we use HPLC to detect melamine in spiked milk samples for comparison to further investigate the performance of the IFE-based fluorescent detection method. As shown in Fig. S8, the retention time of melamine is about 16.4 min. The standard working curve was established with a good linear correlation between peak area and the melamine concentration in the range from 0.8 to 80 $\mu g \cdot mL^{-1}$ ($R^2 = 0.99$), and the detection limit was 0.4 $\mu g \cdot mL^{-1}$ (3σ). Spiked milk samples were determined by HPLC, and the obtained chromatograms were shown in Fig. S9. The recovery of melamine ranged from 85.2% to 98.9% with the variation coefficient of 3.8%–6.3% (Table 1). Then the IFE-based fluorescent method was also applied to determine melamine in spiked milk samples which was diluted 40-fold and the recovery results were listed in Table 2. It can be seen that the recoveries vary from 97.6% to 100.5% with the variation coefficient of 0.8%–1.7%, indicating that the proposed IFE-based fluorescent detection method exhibits remarkable advantages, such as higher sensitivity, less operating time and better reproducibility and preciseness. It demonstrated that this chemosensor can meet the requirements for rapid screening of raw milk samples in a simple way.

Table 2
Application of the proposed method for the determination of melamine in raw milk samples spiked with different amounts of melamine ($n = 3$).

Sample	Concentration of melamine ($mg \cdot L^{-1}$)		Recovery (%)	RSD (%)
	Amount added	Amount found[a]		
Milk 1	0.050	0.049 ± 0.001	97.6	1.3
Milk 2	0.125	0.126 ± 0.002	100.5	1.7
Milk 3	0.250	0.249 ± 0.002	99.4	0.8

[a] Average value of three determinations ± standard deviation.

4. Conclusions

In summary, a sensitive, rapid, simple and economical turn-on fluorescent detection assay for melamine was established using the inner filter effect of AuNPs on L-Cys-capped CdS QDs. Upon addition of CdS QDs to AuNPs, the fluorescence emission of CdS QDs was efficiently decreased due to IFE. When melamine was mixed and incubated with AuNPs before CdS QDs was added, melamine could firstly induce the aggregation of AuNPs and decrease their characteristic surface plasmon absorption, which then resulted in the recovery of IFE-decreased emission of CdS QDs. This detection method showed high precision and sensitivity when applied to determine melamine in raw milk, with a detection limit as low as 0.017 $mg \cdot L^{-1}$, which was much lower than the detection limit of HPLC coupled with UV detector and the safety limit required by USA, UK and China. As no specific modification or labeling step of AuNPs and QDs is involved, the present IFE-based assay allows the design of fluorescent methods in a more rapid and simple way. The required nanomaterials are easily prepared and industrially produced by using some common and low-cost reagents. Compared with traditional methods, the whole procedure including sample pretreatment is promising to be executed by some small-size portable equipments and could be completed within about 30 min, which can save a great deal of manpower, materials and financial resources, and satisfy the needs of supervision departments for on-site rapid monitoring of trace melamine. Therefore, it appears to be a promising selection for rapid screening of melamine contamination in raw milk.

Acknowledgments

This work was financially supported by the National Natural Science Foundation of China (No. 20905031), the Natural Science Foundation of Jilin Province (No. 201215024) and Innovation Projects of Science Frontiers and Interdisciplinary of Jilin University.

Appendix A. Supplementary data

Supplementary data related to this article can be found at http://dx.doi.org/10.1016/j.foodcont.2013.04.016.

References

Ai, K. L., Liu, Y. L., & Lu, L. H. (2009). Hydrogen-bonding recognition-induced color change of gold nanoparticles for visual detection of melamine in raw milk and infant formula. *Journal of the American Chemical Society, 131*, 9496–9497.
Chinese National Standard GB/T 22388-2008. (2008). *Determination of melamine in raw milk and dairy products*. Beijing: Standards Press of China.
Dyadyusha, L., Yin, H., Jaiswal, S., Brown, T., Baumberg, J. J., Booy, F. P., et al. (2005). Quenching of CdSe quantum dot emission, a new approach for biosensing. *Chemical Communications, 25*, 3201–3203.
Gao, F., Ye, Q. Q., Cui, P., & Zhang, L. (2012). Efficient fluorescence energy transfer system between CdTe-doped silica nanoparticles and gold nanoparticles for turn-on fluorescence detection of melamine. *Journal of Agricultural and Food Chemistry, 60*, 4550–4558.
Goodman, W., & Neal-Kababick, J. (2008). *GC–MS screening for melamine adulteration in baby formula and dairy products*. LC GC Europe, 17.
Goscinny, S., Hanot, V., Halbardier, J. F., Michelet, J. Y., & Van Loco, J. (2011). Rapid analysis of melamine residue in milk, milk products, bakery goods and flour by ultra-performance liquid chromatography/tandem mass spectrometry: from food crisis to accreditation. *Food Control, 22*, 226–230.
Grabar, K. C., Brown, K. R., Keating, C. D., Stranick, S. J., Tang, S. L., & Natan, M. J. (1997). Nanoscale characterization of gold colloid monolayers: a comparison of four techniques. *Analytical Chemistry, 69*, 471–477.
Guo, L. Q., Zhong, J. H., Wu, J. M., Fu, F. F., Chen, G. N., Zheng, X. Y., et al. (2010). Visual detection of melamine in milk products by label-free gold nanoparticles. *Talanta, 82*, 1654–1658.

Han, C. P., & Li, H. B. (2010). Visual detection of melamine in infant formula at 0.1 ppm level based on silver nanoparticles. *Analyst, 135*, 583–588.
Khlifi, A., Gam-Derouich, S., Jouini, M., Kalfat, R., & Chehimi, M. M. (2013). Melamine-imprinted polymer grafts through surface photopolymerization initiated by aryl layers from diazonium salts. *Food Control, 31*, 379–386.
Kobayashi, T., Okada, A., Fujii, Y., Niimi, K., Hamamoto, S., Yasui, T., et al. (2010). The mechanism of renal stone formation and renal failure induced by administration of melamine and cyanuric acid. *Urological Research, 38*, 117–125.
Lee, J., Jeong, E. J., & Kim, J. (2011). Selective and sensitive detection of melamine by intra/inter liposomal interaction of polydiacetylene liposomes. *Chemical Communications, 47*, 358–360.
Li, L., Li, B. X., Cheng, D., & Mao, L. H. (2010). Visual detection of melamine in raw milk using gold nanoparticles as colorimetric probe. *Food Chemistry, 122*, 895–900.
Liang, X. S., Wei, H. P., Cui, Z. Q., Deng, J. Y., Zhang, Z. H., You, X. Y., et al. (2011). Colorimetric detection of melamine in complex matrices based on cysteamine-modified gold nanoparticles. *Analyst, 136*, 179–183.
Link, S., & El-Sayed, M. A. (1999). Spectral properties and relaxation dynamics of surface plasmon electronic oscillations in gold and silver nanodots and nanorods. *The Journal of Physical Chemistry B, 103*, 8410–8426.
Lutter, P., Savoy-Perroud, M. C., Campos-Gimenez, E., Meyer, L., Goldmann, T., Bertholet, M. C., et al. (2011). Screening and confirmatory methods for the determination of melamine in cow's milk and milk-based powdered infant formula: validation and proficiency-tests of ELISA, HPLC–UV, GC–MS and LC–MS/MS. *Food Control, 22*, 903–913.
Oh, E., Hong, M. Y., Lee, D., Nam, S. H., Yoon, H. C., & Kim, H. S. (2005). Inhibition assay of biomolecules based on fluorescence resonance energy transfer (FRET) between quantum dots and gold nanoparticles. *Journal of the American Chemical Society, 127*, 3270–3271.
Ping, H., Zhang, M. W., Li, H. K., Li, S. G., Chen, Q. S., Sun, C. Y., et al. (2012). Visual detection of melamine in raw milk by label-free silver nanoparticles. *Food Control, 23*, 191–197.
Qiao, G. H., Guo, T., & Klein, K. K. (2010). Melamine in Chinese milk products and consumer confidence. *Appetite, 55*, 190–195.
Shang, L., & Dong, S. J. (2009). Design of fluorescent assays for cyanide and hydrogen peroxide based on the inner filter effect of metal nanoparticles. *Analytical Chemistry, 81*, 1465–1470.
Shao, N., Zhang, Y., Cheung, S. M., Yang, R. H., Chan, W. H., Mo, T., et al. (2005). Copper ion-selective fluorescent sensor based on the inner filter effect using a spiropyran derivative. *Analytical Chemistry, 77*, 7294–7303.
Sun, H. W., Wang, L. X., Ai, L. F., Liang, S. X., & Wu, H. (2010). A sensitive and validated method for determination of melamine residue in liquid milk by reversed phase high-performance liquid chromatography with solid-phase extraction. *Food Control, 21*, 686–691.
Tang, B., Cao, L. H., Xu, K. H., Zhuo, L. H., Ge, J. H., Li, Q. F., et al. (2008). A new nanobiosensor for glucose with high sensitivity and selectivity in serum based on fluorescence resonance energy transfer (FRET) between CdTe quantum dots and Au nanoparticles. *Chemistry-A European Journal, 14*, 3637–3644.
Wang, X., & Guo, X. Q. (2009). Ultrasensitive Pb^{2+} detection based on fluorescence resonance energy transfer (FRET) between quantum dots and gold nanoparticles. *Analyst, 134*, 1348–1354.
Wang, Y. X., Xiong, L. M., Geng, F. H., Zhang, F. Q., & Xu, M. T. (2011). Design of a dual-signaling sensing system for fluorescent ratiometric detection of Al^{3+} ion based on the inner-filter effect. *Analyst, 136*, 4809–4814.
Weon, B., Rizwana, A., & Rajesh, K. M. (1998). Cysteine-mediated synthesis of CdS bionanocrystallites. *Chemosphere, 37*, 363–385.
Xia, J. G.., Zhou, N. Y., Liu, Y. J., Chen, B., Wu, Y. N., & Yao, S. Z. (2010). Simultaneous determination of melamine and related compounds by capillary zone electrophoresis. *Food Control, 21*, 912–918.
Xu, L., Li, B. X., & Jin, Y. (2011). Inner filter effect of gold nanoparticles on the fluorescence of quantum dots and its application to biological aminothiols detection. *Talanta, 84*, 558–564.
Xu, Y., Wang, Y. M., Wu, J. Z., & Zhang, X. C. (2010). Detecting the melamine of pure milk by near infrared spectra. *Journal of Infrared and Millimeter Waves, 29*, 53–56.
Xue, M., Wang, X., Wang, H., Chen, D. Z., & Tang, B. (2011). Hydrogen bond breakage by fluoride anions in a simple CdTe quantum dot/gold nanoparticle FRET system and its analytical application. *Chemical Communications, 47*, 4986–4988.
Yu, W. W., Qu, L. H., Guo, W. Z., & Peng, X. G. (2003). Experimental determination of the extinction coefficient of CdTe, CdSe, and CdS nanocrystals. *Chemistry of Materials, 15*, 2854–2860.
Zhang, Q., Qu, Y. Y., Liu, M., Li, X. L., Zhou, J. T., Zhang, X. W., et al. (2012). A sensitive enzyme biosensor for catecholics detection via the inner filter effect on fluorescence of CdTe quantum dots. *Sensor and Actuators B: Chemical, 173*, 477–482.
Zhang, X. F., Zou, M. Q., Qi, X. H., Liu, F., Zhu, X. H., & Zhao, B. H. (2010). Detection of melamine in liquid milk using surface-enhanced Raman scattering spectroscopy. *Journal of Raman Spectroscopy, 41*, 1655–1660.
Zhao, W. A., Brook, M. A., & Li, Y. F. (2008). Design of gold nanoparticle-based colorimetric biosensing assays. *ChemBioChem, 9*, 2363–2371.